

Crystal and Molecular Structures of Bis[8-(diphenylphosphino)-quinoline]palladium(II) Complexes: $Pd(Ph_2Pqn)_2XY$ ($XY = Cl_2$, Br_2 or $ClBF_4$)

Takayoshi Suzuki

Department of Chemistry, Graduate School of Science, Osaka University, Toyonaka 560-0043

Received April 30, 2004; E-mail: suzuki@chem.sci.osaka-u.ac.jp

The complex chloride, $Pd(Ph_2Pqn)_2Cl_2$ (Ph_2Pqn = 8-(diphenylphosphino)quinoline), crystallized either in yellow plates (**1a**: from CH_2Cl_2/Et_2O) or in orange needles (**1b**: from $MeOH/Et_2O$). The corresponding bromide, $Pd(Ph_2Pqn)_2Br_2$, initially deposited as yellow block crystals (**2a**) from $MeOH/Et_2O$, turned to orange prisms (**2b**) on standing in the mother liquor. The X-ray crystallographic analyses of **1a** and **2a** revealed that two Cl^- and Br^- anions, respectively, were located above and below the square-planar Pd^{II} coordination plane of *cis*(*P*)-$[Pd(Ph_2Pqn)_2]^{2+}$. Although the distances of Pd···Cl (3.262(3) and 3.386(3) Å) and Pd···Br (3.432(2) and 3.505(2) Å) in **1a** and **2a**, respectively, were too long for a bonding interaction between Pd^{II} and X^-, weak Pd^{II}···X^- charge-transfer interactions seem to be responsible for the yellow colors of these crystals. In contrast, in **2b**, the Pd^{II} formed an elongated square-pyramidal five-coordinate complex, $[Pd(Ph_2Pqn)_2Br]^+$, with a somewhat long Pd–Br bond (3.0136(8) Å) at the apical position. The crystal structure of $Pd(Ph_2Pqn)_2ClBF_4$ (**4**) revealed that the Pd^{II} center in **4** took an extremely distorted square-planar coordination geometry with the Pd–Cl bond of 2.375(2) Å, while one of the Ph_2Pqn ligands coordinated through only P; *cis*(*P*)-[PdCl(Ph_2Pqn-κP,*N*)(Ph_2Pqn-κP)]BF_4.

Phosphines bearing an 8-quinolyl substituent (R_2Pqn: Scheme 1) can act as asymmetrical bidentate ligands to form a planar five-membered chelate ring and may stabilize unusual oxidation state and/or coordination geometry of the metal ions upon coordination, owing to the steric requirements and the electronic differentiation of the phosphino and quinolyl donor groups.[1,2] It has also been reported that their ruthenium(II) complexes, $[Ru(bpy \text{ or } phen)_2(R_2Pqn)]^{2+}$, exhibited novel dual emission, since the quinolyl moiety in R_2Pqn gave a characteristic long-lived $^3(\pi$–$\pi^*)$ emission.[3] Furthermore, some nickel(II) and palladium(II) complexes coordinated by R_2Pqn showed catalytic activities toward ethylene polymerization or reductive carbonylation of nitrobenzene.[4,5] However, fundamental studies on structures and electronic properties of the R_2Pqn complexes have not been well developed,[1–9] compared with the metal complexes containing other asymmetrical bidentate P–N type ligands;[6] of all reported palladium(II) complexes, such as $PdCl_2(Ph_2Pqn)$ by Tayim et al.,[2] $[Pd(Ph_2Pqn)_2](PF_6)_2$ by van Leeuwen et al.,[5] $PdCl_2(PhMePqn)$, $[Pd(C\text{–}N)(PhMePqn)]PF_6$ (C–N = dimethyl(1-ethyl-α-naphthyl)amino-C^2,*N*), $[PdCl(PhMePqn)_2]Cl$, and $[Pd(PhMePqn)_2](PF_6)_2$ by Salem and Wild,[7,8] and $PdX_2(Me_2Pqn)$ (X = Cl, Br, and I) and *cis*(*P*)-$[Pd(Me_2Pqn)_2](BF_4)_2$ by us,[1] only two complexes, $[Pd(C\text{–}N)(PhMePqn)]PF_6$[7] and *cis*(*P*)-$[Pd(Me_2Pqn)_2](BF_4)_2$, have been structurally characterized by the single-crystal X-ray analysis. In the colorless crystal of *cis*(*P*)-$[Pd(Me_2Pqn)_2](BF_4)_2$, the Pd^{II} center took a square-planar coordination geometry with two chelated Me_2Pqn ligands in the *cis*(*P*) configuration. However, the quinolyl planes were bent away from the Pd^{II} coordination plane by the interligand steric interaction between mutually *cis*-positioned quinolyl groups.[1] For analogous Ph_2Pqn and PhMePqn complexes, $[Pd(Ph_2Pqn \text{ or } PhMePqn)_2](PF_6)_2$, which were also isolated as colorless crystals, similar *SP*-4-22 (= *cis*(*P*)) molecular structures were suggested by NMR spectroscopy.[5,8] In contrast to the colorless BF_4^- or PF_6^- salts of $[Pd(R_2Pqn)_2]^{2+}$, the halide salts ($Pd(R_2Pqn)_2X_2$; X = Cl (**1**), Br (**2**), or I (**3**)) appear yellow or red (Fig. 1). Although a five-coordinate square-pyramidal structure was indicated for the yellow $[PdCl(PhMePqn)_2]Cl$ complex on the basis of the ^1H NMR study by Salem and Wild,[8] no explicit evidence such as the crystal structure has been reported so far. In this study, we have succeeded in determining the crystal structures of **1**, **2**, and $[Pd(Ph_2Pqn)_2Cl]BF_4$ (**4**), and the structures of these complexes in solution were determined on the basis of ^{31}P NMR and UV–vis measurements.

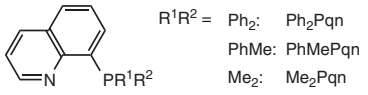

Scheme 1. 8-Quinolylphosphines.

Experimental

Preparation of Complexes. The ligand Ph_2Pqn was prepared according to the method described by Feltham and Metzger,[10] and handled under an atmosphere of nitrogen until it formed air-stable palladium(II) complexes. The complex, $PdCl_2(PhCN)_2$, was prepared by the literature method.[11]

$Pd(Ph_2Pqn)_2Cl_2$ (1): A CH_2Cl_2 solution (10 cm^3) of $PdCl_2(PhCN)_2$ (580 mg, 1.50 mmol) was added dropwise with stirring to a CH_2Cl_2 solution (15 cm^3) of Ph_2Pqn (939 mg, 3.00 mmol). After stirring at ambient temperature for 4 h, the mixture was evaporated under reduced pressure. The orange oily residue was thoroughly washed with Et_2O (100 cm^3) to give orange powders.

Published on the web October 9, 2004; DOI 10.1246/bcsj.77.1869

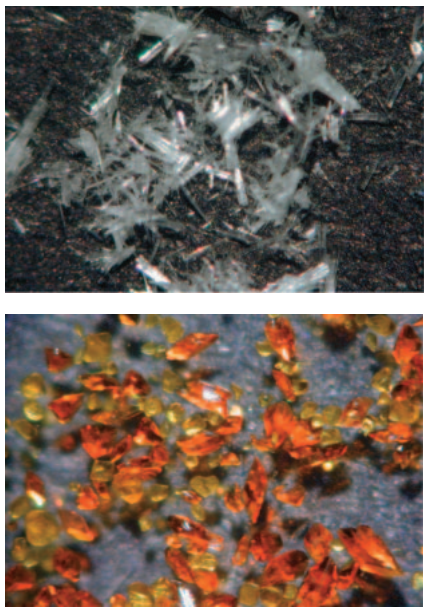

Fig. 1. (a) Colorless needle crystals of *cis*-$[Pd(Ph_2Pqn)_2](BF_4)_2$ (**5**) deposited from MeOH/CH_3CN. (b) Yellow block crystals (**2a**) and orange prismatic crystals (**2b**) of $Pd(Ph_2Pqn)_2Br_2$ obtained from MeOH/Et_2O (a part of yellow **2a** converted to orange **2b** on leaving them in the mother liquor for a week: see text).

The crude product was recrystallized by vapor diffusion of Et_2O into a CH_2Cl_2 solution, affording yellow plate crystals of **1a** (= **1**·$2CH_2Cl_2$·H_2O). Yield: 967 mg (0.975 mmol, 65%). Anal. Found: C, 54.04; H, 4.11; N, 3.00%. Calcd for $C_{44}H_{38}Cl_6N_2OP_2Pd$: C, 53.28; H, 3.86; N, 2.82%. When this compound was recrystallized from MeOH by vapor diffusion of Et_2O, orange needle crystals (**1b**) were deposited. These crystals were highly efflorescent, and turned into yellow powder immediately after filtration from the mother liquor.

$Pd(Ph_2Pqn)_2Br_2$ (2) and $Pd(Ph_2Pqn)_2I_2$ (3): To a $CHCl_3$ solution (15 cm^3) of **1a** (200 mg, 0.202 mmol) was added a MeOH solution (15 cm^3) of KBr (200 mg, 1.68 mmol); the mixture was stirred overnight at ambient temperature. After evaporation of the solvent under reduced pressure, the residue was extracted with CH_2Cl_2 (50 cm^3). The extract was concentrated (to 5 cm^3) by evaporation, and the vapor of Et_2O was diffused into the concentrate, giving orange needle crystals of **2**·$2CH_2Cl_2$. Yield: 177 mg (0.167 mmol, 83%). Anal. Found: C, 49.85; H, 3.51; N, 2.70%. Calcd for $C_{44}H_{36}Br_2Cl_4N_2P_2Pd$: C, 49.72; H, 3.41; N, 2.64%. When this compound was recrystallized from MeOH/Et_2O, yellow block crystals (**2a**) were first deposited. However, these crystals converted into orange prismatic crystals (**2b**) on leaving them in the mother liquor for several weeks (Fig. 1b). The complex iodide was prepared in a similar way by using KI to afford red plate crystals of **3**·H_2O. Yield: 86%. Anal. Found: C, 50.14; H, 3.28; N, 2.79%. Calcd for $C_{42}H_{34}I_2N_2OP_2Pd$: C, 50.20; H, 3.41; N, 2.79%.

$[Pd(Ph_2Pqn)_2](BF_4)_2$ (5): To a MeOH solution (160 cm^3) of **1a** (328 mg, 0.331 mmol) was added a MeOH solution (10 cm^3) of $AgBF_4$ (159 mg, 0.815 mmol). After stirring at ambient temperature for 2 h, the mixture was evaporated to dryness under reduced pressure. The residue was extracted with CH_3CN (100 cm^3), and the extract was evaporated to dryness. The obtained white powder was recrystallized from a mixture of MeOH and CH_3CN to give colorless needle crystals of **5** (Fig. 1a). Yield: 249 mg (0.275 mmol, 83%). Anal. Found: C, 55.40; H, 3.66; N, 3.23%. Calcd for $C_{42}H_{32}B_2F_8N_2P_2Pd$: C, 55.64; H, 3.56; N, 3.09%.

$[Pd(Ph_2Pqn)_2Cl]BF_4$ (4): This complex was prepared by the addition of an equimolar amount of $AgBF_4$ to $Pd(Ph_2Pqn)_2Cl_2$. Orange prismatic crystals of **4**·MeOH were obtained by recrystallization from a mixture of MeOH and CH_3CN. Yield: 60%. Anal. Found: C, 58.19; H, 3.93; N, 3.50%. Calcd for $C_{43}H_{36}BClF_4N_2OP_2Pd$: C, 58.20; H, 4.09; N, 3.16%.

Crystallography. Each crystal of **1a**, **2b**, and **4**·MeOH suitable for the X-ray diffraction study was sealed in a glass capillary tube. The X-ray diffraction data (up to $2\theta = 55^\circ$) were measured at 23(2) °C on a Rigaku AFC-5R four circle diffractometer equipped with a graphite-monochromated Mo K_α radiation (λ = 0.71073 Å). Final lattice parameters were determined by least-squares treatment using setting angles of 25 reflections in the range of $25 < 2\theta < 30^\circ$. The intensities were corrected for Lorentz-polarization factors and for absorption effects by the numerical integration method.[12] As the yellow crystals of **2a** were highly efflorescent when they were picked up from the mother liquor, the crystal was mounted with a cryoloop and flash-cooled by the cold nitrogen steam. The diffraction data of **2a** were obtained at −100(2) °C on a Rigaku R-axis rapid imaging plate detector with a graphite-monochromated Mo K_α radiation (λ = 0.71073 Å). A total of 110 images with the oscillation angle of $\omega = 2^\circ$ were collected with 2 different goniometer settings ($8 < 2\theta < 55^\circ$, exposure time = 300 s ω^{-1}). Data were processed by the Process-Auto program package,[13] and the lattice parameters were determined by least-squares treatment using setting angles of all reflections observed. Absorption corrections were applied by the empirical method.[14]

The structures were solved either by the direct method using SIR92[15] or by the heavy-atom method using SHELXS86 program,[15] and refined on F^2 (with all independent reflections) using SHELXL97 program.[16] In the crystal of **2a**, some solvated molecules were observed, all of which were assumed to be methanol; $Pd(Ph_2Pqn)_2Br_2$·4.5MeOH. Except for the solvated molecules of **2a**, all non-H atoms were refined anisotropically, and H atoms were introduced at the positions calculated theoretically and treated with riding models. All calculations were carried out using the teXsan software package.[17]

Crystal data are collected in Table 1, and selected bond lengths and angles are listed in Table 2.

Measurements. UV–vis absorption spectra were measured at 20 °C on a Perkin-Elmer Lambda 19 spectrophotometer. The spectra of solid compounds in the form of Nujol mulls were obtained according to the method described by Lee et al.[18] The variable-temperature ^{31}P NMR spectra were acquired on a Jeol Lambda 500 spectrometer, and the chemical shifts were referenced from external 85% H_3PO_4 (δ 0).

Results and Discussion

Syntheses and Crystal Structures. A reaction of $PdCl_2(PhCN)_2$ and two equivalent amounts of Ph_2Pqn in CH_2Cl_2 at room temperature gave a clear yellow-orange solution. During this reaction, a yellow precipitate of $PdCl_2(Ph_2Pqn)$ was initially formed.[2] However, this precipitate redissolved completely when all Ph_2Pqn was added. From this solution, orange powder was obtained by evaporation of the solvent. This product crystallized either in yellow plates of $Pd(Ph_2Pqn)_2Cl_2$·$2CH_2Cl_2$·H_2O (**1a**) from CH_2Cl_2, or in or-

Table 1. Crystallographic Data for $Pd(Ph_2Pqn)_2Cl_2 \cdot 2CH_2Cl_2 \cdot H_2O$ (**1a**), $Pd(Ph_2Pqn)_2Br_2 \cdot nCH_3OH$ (**2a**, $n = 4.5$; **2b**, $n = 1$), and $[Pd(Ph_2Pqn)_2Cl]BF_4 \cdot MeOH$ (**4**·MeOH)

Compound	**1a**	**2a**	**2b**	**4**·MeOH
Formula	$C_{44}H_{38}Cl_6N_2OP_2Pd$	$C_{46.5}H_{41}Br_2N_2O_{4.5}P_2Pd$	$C_{43}H_{36}Br_2N_2OP_2Pd$	$C_{43}H_{36}BClF_4N_2OP_2Pd$
FW	991.80	1027.97	924.90	887.34
T/K	296(2)	173(2)	296(2)	296(2)
Crystal color, shape	yellow, plate	yellow, block	orange, prism	orange, plate
Crystal dimension/mm	$0.20 \times 0.18 \times 0.08$	$0.12 \times 0.10 \times 0.06$	$0.28 \times 0.26 \times 0.24$	$0.26 \times 0.24 \times 0.08$
Crystal system	triclinic	monoclinic	monoclinic	monoclinic
Space group, Z	$P\bar{1}$, 2	$I2/a$, 8	$P2_1/n$, 4	$P2_1/a$, 4
a/Å	11.178(4)	17.348(11)	13.3506(13)	17.630(5)
b/Å	13.122(3)	30.05(2)	17.4049(17)	14.218(4)
c/Å	15.086(6)	17.856(13)	16.473(2)	17.906(4)
α/deg	98.01(3)	90	90	90
β/deg	101.87(3)	91.07(6)	90.753(10)	118.68(1)
γ/deg	93.17(3)	90	90	90
V/Å^3	2136(1)	9308(11)	3827.4(7)	3938(2)
D_x/Mg m^{-3}	1.542	1.467	1.605	1.497
$F(000)$	1004	4128	1848	1800
μ(Mo Kα)/mm^{-1}	0.922	2.228	2.693	0.676
T_{min}, T_{max}	0.830, 0.911	0.487, 0.836	0.481, 0.585	0.826, 0.945
Refln/param ratio	9830/505	10532/486	8800/460	8948/496
$R1$ [$F_o^2 > 2\sigma(F_o^2)$]	0.056	0.076	0.045	0.048
$wR2$ (all refln)	0.191	0.197	0.119	0.163
GoF	1.003	0.994	1.018	1.026

Table 2. Selected Bond Lengths and Angles

Compound	**1a**	**2a**	**2b**	**4**·MeOH
Pd···Cl(1) [Pd···Br(1)]	3.262(3)	[3.432(2)]	[3.0136(8)]	2.375(2)
Pd···Cl(2) [Pd···Br(2)	3.386(3)	[3.505(2)]	[4.423(1)]	—
Pd–P(1)	2.229(2)	2.234(2)	2.241(1)	2.241(2)
Pd–P(2)	2.232(2)	2.240(2)	2.240(1)	2.267(2)
Pd–N(1)	2.139(4)	2.128(6)	2.179(4)	2.100(5)
Pd–N(21) [Pd···N(21)]	2.135(4)	2.148(6)	2.107(4)	[2.725(7)]
P(1)–Pd–P(2)	97.65(7)	97.42(8)	98.80(5)	100.01(6)
P(1)–Pd–N(1)	82.5(1)	81.7(2)	81.4(1)	84.0(1)
P(2)–Pd–N(21) [P(2)–Pd···N(21)]	82.3(1)	81.5(2)	84.2(1)	[70.8(1)]
P(1)–Pd–N(21) [P(1)–Pd···N(21)]	171.0(1)	171.5(2)	175.9(1)	[119.2(2)]
P(2)–Pd–N(1)	169.8(1)	173.7(2)	157.6(1)	172.5(2)
N(1)–Pd–N(21) [N(1)–Pd···N(21)]	99.1(2)	100.3(2)	96.9(2)	[101.7(2)]

ange needles (**1b**) from MeOH, by vapor diffusion of Et_2O. The orange crystals of **1b** were highly efflorescent; they turned to yellow powder within a few seconds after filtration from the mother liquor. The complex, either **1a** or **1b**, reacted with two equivalent amounts of $AgBF_4$ (or excess amounts of $LiBF_4$) to give a colorless complex of $[Pd(Ph_2Pqn)_2](BF_4)_2$ (**5**), which crystallized in colorless needles (Fig. 1a). The coordination geometry of colorless complex **5** has been assumed to be square-planar with *cis*(*P*) configuration on the basis of the NMR results (vide infra), and from the crystal structure of the analogous Me_2Pqn complex, *cis*(*P*)-$[Pd(Me_2Pqn)_2](BF_4)_2$.[1] Therefore, it is interesting to elucidate the crystal structure of $Pd(Ph_2Pqn)_2Cl_2$ (**1**), since crystals of **1** are colored yellow (**1a**) or orange (**1b**) depending on the solvent used for crystallization.

The X-ray analysis for **1a** revealed that the Pd^{II} center is in a slightly distorted square-planar coordination geometry with two chelating Ph_2Pqn ligands in the *cis*(*P*) configuration (Fig. 2). The Pd–P and Pd–N bond lengths are in the range of 2.229(2)–2.232(2) and 2.135(4)–2.139(4) Å, respectively, which are comparable to those in *cis*(*P*)-$[Pd(Me_2Pqn)_2](BF_4)_2$.[1] Due to the interligand steric interaction between the *ortho*-H atoms of the mutually *cis*-positioned quinolyl rings, the quinolyl planes were not coplanar with the Pd^{II} coordination plane; the dihedral angles between the least-squares PdP_2N_2 plane and the quinolyl planes were 16.4(1) and 15.5(1)°, and the dihedral angle between two quinolyl planes was 26.2(1)°. Thus, the structure of $Pd(R_2Pqn)_2$ moiety in **1a** is very similar to that in *cis*(*P*)-$[Pd(Me_2Pqn)_2](BF_4)_2$.[1] In **1a** two Cl^- anions were placed above and below the Pd^{II} coordination plane with the distances of 3.262(3) and 3.386(3) Å for Pd···Cl(1) and Pd···Cl(2), respectively. These Pd···Cl distances are rather long compared with the typical Pd–Cl coordination bond (~2.3 Å)[19] and are still longer than the Pd···Cl distance

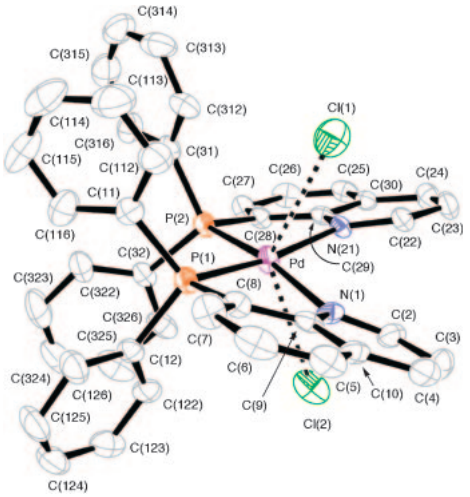

Fig. 2. ORTEP (30% probability level) of the $Pd(Ph_2Pqn)_2Cl_2$ part in **1a**. Hydrogen atoms are omitted for clarity.

found in *cis*-$[Pd(Me_2PCH_2CH_2NH_2)_2]Cl(BF_4)$ (3.156(3) Å).[20] In addition, the Cl atoms were displaced from the apex positions of an ideal octahedron, Cl(1)···Pd···Cl(2) 141.60(6)°; this was due probably to the steric hinderance of the phenyl groups on the P atoms. We conclude that there is no explicit bonding interaction between Pd^{II} and Cl^-, while the yellow color of crystals **1a** certainly indicates the existance of charge-transfer interaction between Pd^{II} and Cl^-.

Metathesis reactions of $Pd(Ph_2Pqn)_2Cl_2$ (**1**) with KBr and with KI in a mixture of $CHCl_3$ and MeOH produced the corresponding bromide and iodide complexes, $Pd(Ph_2Pqn)_2Br_2$ (**2**) and $Pd(Ph_2Pqn)_2I_2$ (**3**), respectively. The iodide complex **3**, which was deposited as red thin-plate crystals of $\mathbf{3}\cdot H_2O$ from CH_2Cl_2/Et_2O, was well soluble in CH_2Cl_2, while it was hardly soluble in MeOH. On the other hand, the bromide complex **2** was very soluble in both CH_2Cl_2 and MeOH. When complex **2** was recrystallized from a CH_2Cl_2 solution by vapor diffusion of Et_2O, orange needle crystals ($\mathbf{2}\cdot 2CH_2Cl_2$) were deposited. In contrast, from MeOH/Et_2O complex **2** crystallized at first in yellow blocks (**2a**), which turned to orange prisms (**2b**) when the crystals were kept in the mother liquor for several weeks (Fig. 1b). The crystals of **2a** are highly efflorescent, while those of **2b** are relatively stable in the air.

We also succeeded in the analyses of the crystal structures of both **2a** ($Pd(Ph_2Pqn)_2Br_2\cdot 4.5MeOH$ at −100 °C) and **2b** ($Pd(Ph_2Pqn)_2Br_2\cdot MeOH$ at 23 °C). As seen in Fig. 3a, the structure of the $Pd(Ph_2Pqn)_2Br_2$ moiety in **2a** is similar to that of $Pd(Ph_2Pqn)_2Cl_2$ in **1a**. The Pd···Br distances in **2a** are as follows; Pd···Br(1) 3.432(2) and Pd···Br(2) 3.505(2) Å. The Pd–P and Pd–N bond lengths are 2.234(2)–2.240(2) and 2.128(6)–2.148(6) Å, respectively, which are consistent with those in **1a**. The dihedral angles between the least-squares PdP_2N_2 plane and each quinolyl plane were 19.9(1) and 18.5(1)°, and the dihedral angle between two quinolyl planes was 26.4(2)°.

In the orange prismatic crystals of **2b**, two Ph_2Pqn ligands coordinated to the Pd^{II} center via P and N atoms to form a five-membered chelate ring in the mutually *cis* configuration (Fig. 3b), like those in **1a** and **2a**. On the other hand, the coordination structures of two Ph_2Pqn ligands in **2b** were found to

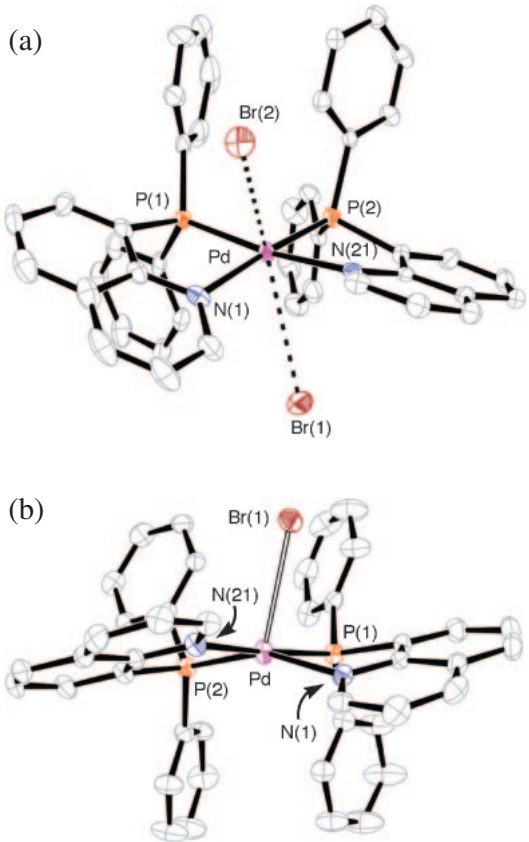

Fig. 3. ORTEPs (30% probability level) of (a) the $Pd(Ph_2Pqn)_2Br_2$ part in **2a** and (b) the $[Pd(Ph_2Pqn)_2Br]^+$ part in **2b**. Hydrogen atoms are omitted for clarity.

be dissimilar to each other. Although two Pd–P bond lengths were the same (Pd–P(1) 2.241(1) Å and Pd–P(2) 2.241(1) Å), Pd–N(1) (2.179(4) Å) was relatively longer than Pd–N(21) (2.107(4) Å). In relation to this discrepancy of the Pd–N bond lengths, the quinolyl plane containing N(21) was almost coplanar with the least-squares PdP_2N_2 plane[21] (the dihedral angle, 9.36(8)°), while the other quinolyl ring including N(1) is largely bent away from the Pd^{II} coordination plane (the dihedral angle, 24.20(9)°). The most striking difference between the crystal structures of **2a** and **2b** was the position of Br^- anions; in **2b**, Br(1) was found at the position closer to the Pd^{II} center (Pd···Br(1) 3.0136(8) Å), while the other Br(2) was far more distant from Pd^{II} (Pd···Br(2) 4.403(1) Å). Although the Pd···Br(1) distance was still longer than the typical Pd^{II}–Br coordination bond lengths (~2.45 Å),[19] a bonding interaction between Pd and Br(1) was suggested to some extent. Therefore, the coordination geometry around Pd^{II} in **2b** may be described as an elongated five-coordinate square-pyramid, (*SPY*-5-13)-$[Pd(Ph_2Pqn\text{-}\kappa P,N)_2Br]^+$. It is also possible to describe this coordination structure as a distorted trigonal bipyramid,[21] because of the P(2)–Pd–N(1) bond angle (157.6(1)°). Similar elongated five-coordinate square-pyramidal structures have been reported for $[Pd(Ph_2P(CH_2)_2PPh\text{-}(CH_2)_2P(O)Ph_2\text{-}\kappa P,P)_2Br]Br$[22] and [Pd(5-ethyl-5*H*-dibenzophosphole or 2-phenylisophosphindoline)$_3Br_2$],[23] where the Pd–Br(apical) bond lengths were 2.898(2) and 2.923(3)–3.017(2) Å, respectively. The former complex is yellow, which

is an interesting analogy to complex **2**; [Pd($Ph_2P(CH_2)_2PPh$-$(CH_2)_2P(O)Ph_2$-$\kappa P,P)_2$Br]Br is yellow in color, while the square-planar $[Pd^{II}(phosphine)_4]^{2+}$ type complexes usually form colorless crystals.[24] Hence, the orange color of **2b** may result from a stronger charge-transfer interaction between Pd^{II} and Br^- (vide infra). A red crystal of the five-coordinate trigonal bipyramidal Pd^{II} complex having a tripodal tetradentate phosphine, [Pd{$P(CH_2CH_2PPh_2)_3$}Br]Br, has also been structurally analyzed; here the Pd–Br bond is much shorter, 2.517(2) Å.[25]

It was also possible to isolate orange prismatic crystals of $Pd(Ph_2Pqn)_2Cl(BF_4)\cdot$MeOH (**4**·MeOH) by a reaction of **1a** and an equimolar amount of $AgBF_4$. Although we expected formation of an elongated square pyramidal $[Pd(Ph_2Pqn)_2Cl]^+$, such as the bromo complex in **2b**, the structural analysis of **4** revealed that this complex has a highly distorted square-planar geometry around Pd^{II} center with a chelating Ph_2Pqn, a monodentate P-donating Ph_2Pqn and a Cl^- ion: *cis*(*P*)-[Pd(Ph_2Pqn-$\kappa P,N$)(Ph_2Pqn-κP)Cl]$^+$ (Fig. 4). The Pd–Cl(1) bond length was 2.375(2) Å and the Pd–P lengths were in the range of 2.241(2)–2.267(2) Å. The Pd–N(1), 2.100(5) Å, was slightly shorter than those in **1a** and **2a**, but comparable to the Pd–N(21) bond in **2b**, the latter of which resulted from the reduction of the interligand steric hinderance between quinolyl moieties. The dihedral angle between the quinolyl plane in the chelated Ph_2Pqn and the plane defined by Pd, P(1), P(2), and N(1) was 10.5(1)°. The N(21) atom was apart from the Pd^{II} center by 2.725(7) Å, and the quinolyl plane containing N(21) had a dihedral angle of 49.8(1)° relative to the $Pd^{II}P_2N$ plane. Thus, we concluded that there is no bonding interaction between Pd and N(21) in **4**. However, it is also possible to consider that the coordination geometry around Pd^{II} center is closely related to trigonal bipyramidal, since Cl(1) is also largely displaced (0.934(3) Å) from the $Pd^{II}P_2N$ plane (P(1)–Pd–Cl(1) 156.14(6)°).

Absorption Spectra in the Solid States. In order to clarify the color-change of the crystals due to the exchange of anions, the absorption spectra of $Pd(Ph_2Pqn)_2XY$ (**1**–**5**) in the solid state were examined. The complex of *cis*-$[Pd(Ph_2Pqn)_2](BF_4)_2$ (**5**), which has no absorption in the visible (>400 nm) region as inferred from its colorless crystals, showed an intense band at 310 nm accompanied by a shoulder around 360 nm (Fig. 5a).

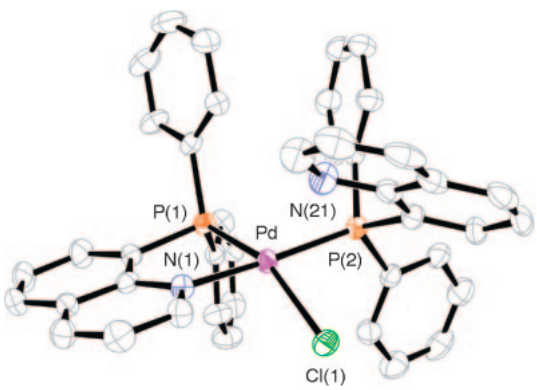

Fig. 4. ORTEP (30% probability level) of the cationic part in $[Pd(Ph_2Pqn)_2Cl]BF_4\cdot$MeOH (**4**·MeOH). Hydrogen atoms are omitted for clarity.

The absorption band at 310 nm may be assigned as the intraligand π–π^* transition of the quinolyl moiety, since free Ph_2Pqn also shows a similar intense band at the same energy region. Then, the shoulder at ca. 360 nm may be due to the phosphine-to-Pd^{II} charge-transfer band, as the corresponding shoulder for *cis*-$[Pd(Me_2Pqn)_2](BF_4)_2$ was blue-shifted to ca. 330 nm.[1]

As described above, the $Pd(Ph_2Pqn)_2Cl_2$ complex crystallized either in yellow plates (**1a**) or in orange needles (**1b**), and crystals of **1b** turned to yellow powder immediately after filtration in the air. The powder samples of **1a** and **1b** (yellow) did not exhibit significant difference in their absorption spectra; both spectra showed an intense band at 310 nm accompanied by a broad shoulder around 420 nm. The yellow crystals of the bromide complex (**2a**) exhibited a similar spectrum, but the broad shoulder became further red-shifted to ~440 nm. As the X-ray crystal structure analyses revealed that $[Pd(Ph_2Pqn)_2]^{2+}$ moieties in **1a** and **2a** have structures similar to each other (and probably to that in **5**), the observed absorption shoulder in the visible region seems to have originated from the charge-transfer interaction between Pd^{II} and halide anions.

The orange crystals of **2b** gave an explicit absorption band at 450 nm (Fig. 5b); it was observed at the energy region lower than the absorption shoulder of the yellow crystals of **2a**. As seen in the crystal structure analyses, the Pd^{II} forms a five-coordinate square-pyramidal complex with a Pd–Br bond of 3.0136(8) Å in **2b**, while the Pd···Br distances are 3.432(2) and 3.505(2) Å in **2a**. In addition to the distortion toward trigonal bipyramidal geometry, the stronger Pd–Br interaction in **2b** causes a lower energy shift of the Br^--to-Pd^{II} charge-transfer band.

The spectrum of **4** is shown in Fig. 5a. We expected a different absorption spectrum for **4** from that of **1a** at least in the solid states, since the coordination geometry around the Pd^{II} center in **4**·MeOH is found to be different from that in **1a**. Although the spectrum of **4** seems to have a lower-energy should-

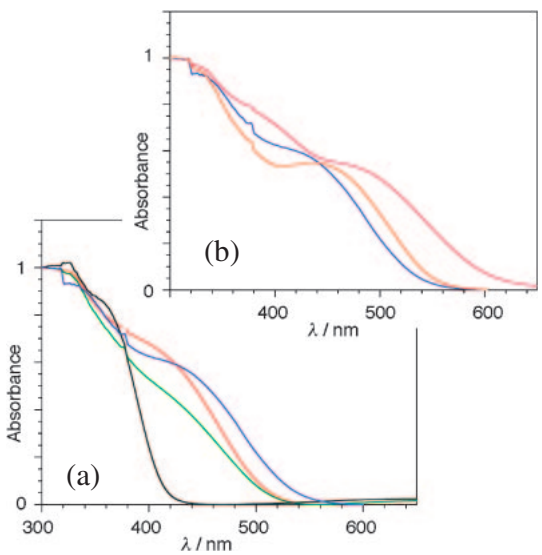

Fig. 5. Normalized absorption spectra of (a) **5** (black), **4** (green), **2a** (blue), and **1a** (red); and (b) **2a** (blue), **2b** (orange), and **3** (purple) in the solid states.

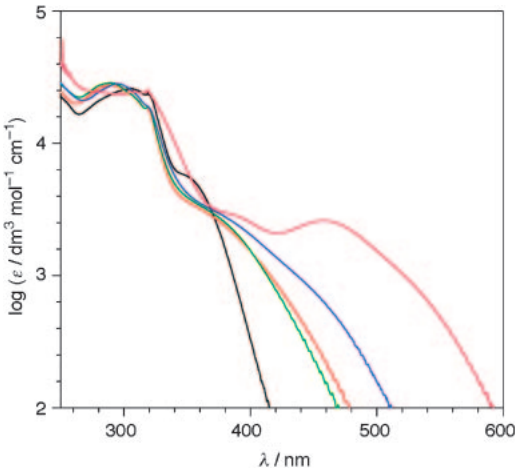

Fig. 6. Absorption spectra of **1** (red), **2** (blue), and **3** (purple) in CH_2Cl_2, **4** (green) and **5** (black) in CH_3CN at room temperature.

er in energy region that corresponds to the charge-transfer transition, no other explicit differences were observed between the absorption spectra of **4** and **1a**.

Structures in Solution. The complex **5** exists as *cis*-$[Pd(Ph_2Pqn)_2]^{2+}$ in acetonitrile; the ^{31}P NMR spectrum of **5** in CD_3CN (30 °C) showed a sharp single resonance at δ 50.7, which is consistent with the value reported for the analogous complex, *cis*-$[Pd(Ph_2Pqn)_2](PF_6)_2$.[5] The UV–vis spectrum of **5** in CH_3CN (~0.1 mM) showed an intense absorption band at 304 nm accompanied by a shoulder around 350 nm (Fig. 6), which is similar to the spectrum in the solid state.

Complexes of $Pd(Ph_2Pqn)_2Cl_2$ (**1**) and $Pd(Ph_2Pqn)_2Br_2$ (**2**), irrespective of their crystal forms (i.e., yellow **1a**/**2a** or orange **1b**/**2b**), are well soluble in methanol and dichloromethane, and the UV–vis and ^{31}P NMR spectra of these complexes are apparently solvent-dependent. In MeOH (~0.1 mM) both complexes **1** and **2** exhibited similar UV–vis absorption spectra (not shown in Fig. 6 for clarity) to that of **5** in CH_3CN; there were no absorptions in the visible (>400 nm) region. The ^{31}P NMR spectra of **1** and **2** in CD_3OD (at 30, −40, and −80 °C) showed a sharp single resonance with a similar chemical shift to that for **5** (Table 3). Thus, these complexes in methanol exist as *cis*-$[Pd(Ph_2Pqn)_2]^{2+}$ with no detectable interaction between the square-planar Pd^{II} center and halide anions. In contrast, the UV–vis absorption spectrum of **1** in CH_2Cl_2 was obviously different from that of **5** in CH_3CN, but was very similar to the spectrum of **4** in CH_3CN (Fig. 6). These spectra of **1** (in CH_2Cl_2) and **4** (in CH_3CN) showed an intense absorption band at 289 nm accompanied by a broad shoulder around 370 nm, which was responsible to the yellow color of the solutions. The complex **2** in CH_2Cl_2 gave a similar absorption spectrum, but the shoulder was further red-shifted by 10–20 nm. These facts indicate that in dichloromethane or acetonitrile there is an explicit charge-transfer interaction between the Pd^{II} center and the halide anion (Cl^- or Br^-).

The ^{31}P NMR spectrum of **4** in CD_3CN at 30 °C showed a sharp single resonance at δ 36.7, which was inconsistent with the crystal structure of the complex, *cis*(*P*)-$[PdCl(Ph_2Pqn$-$\kappa P,N)(Ph_2Pqn$-$\kappa P)]^+$. However, the higher field shift compared with that of **5**, and the broader linewidth with a slightly

Table 3. ^{31}P NMR Chemical Shift (δ) and Its Half-Height Width ($\Delta_{1/2}$) of Complexes

Complex	Solvent	Temp./°C	δ	$\Delta_{1/2}$/Hz
$Pd(Ph_2Pqn)_2Cl_2$	CD_3OD	30	49.4	<20
		−40	50.6	<20
		−80	50.9	<20
	CD_2Cl_2	30	36.1	<20
		−40	37.3	~110
		−80	40.3	~1100
$Pd(Ph_2Pqn)_2Br_2$	CD_3OD	30	49.3	<20
		−40	50.1	<20
		−80	50.2	<20
	CD_2Cl_2	30	38.3	<20
		−80	47.8	~100
$Pd(Ph_2Pqn)_2I_2$	CD_2Cl_2	30	41.8	~180
		−40	46.5	<20
		−80	47.8	<20
$Pd(Ph_2Pqn)_2ClBF_4$	CD_3CN	30	36.7	<20
		−40	39.3	~130
$Pd(Ph_2Pqn)_2(BF_4)_2$	CD_3CN	30	50.7	<20

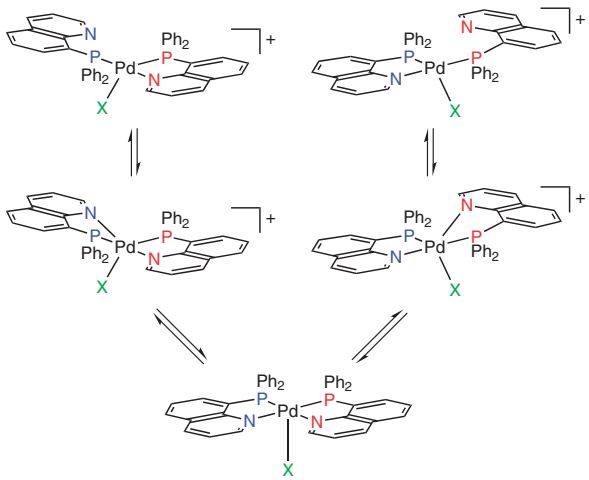

Scheme 2.

down-field shift at −40 °C (Table 3), indicate that the complex **4** exists as a monocationic complex, $[PdCl(Ph_2Pqn)_2]^+$, with two chemically equivalent P atoms in CD_3CN. The observed temperature-dependence of the linewidth and the chemical shift indicate a rapid exchange equilibrium of the chelating and monodentate P-donating Ph_2Pqn ligands in the (distorted) square-planar complex of *cis*(*P*)-$[PdCl(Ph_2Pqn$-$\kappa P,N)(Ph_2$-Pqn-$\kappa P)]^+$ (Scheme 2). The VT ^{31}P NMR spectra of **1** and **2** in CD_2Cl_2 gave similar characteristics to those observed for complex **4**; at −80 °C these solutions gave a very broad signal at δ 40.3 and 47.8, respectively (Table 3). Therefore, complexes **1** and **2** exist as a monocationic complex having a Pd–Cl or Br bond in dichloromethane solutions and exhibit a fluxionality due probably to the exchange equilibrium described in Scheme 2.[26]

The complex $Pd(Ph_2Pqn)_2I_2$ (**3**) in CH_2Cl_2 showed intense absorption bands at 380 and 457 nm, which were characteristic of this complex (Fig. 6). In the ^{31}P NMR spectrum of **3** in

CD_2Cl_2 at 30 °C a broad signal was observed at δ 41.8. Interestingly, this signal became sharp by lowering the temperature of the sample solution; at −40 °C a sharp single signal was observed at δ 46.5. These observations indicate the stabilization of the square-pyramidal five-coordinate complex of $[PdI(Ph_2Pqn\text{-}\kappa P,N)_2]^+$ in CD_2Cl_2 at low temperatures. Otherwise, a neutral species, i.e., $[PdI_2(Ph_2Pqn\text{-}\kappa P)_2]$ may exist in solution, and (one of) the quinolyl-N atoms become coordinated to the Pd^{II} center, giving a fluxional behavior with increasing the temperature.

Conclusion

In this study we have determined the structures of $Pd(Ph_2Pqn)_2XY$ (XY = Cl_2 (**1**), Br_2 (**2**), and $ClBF_4$ (**4**)) in the solid states and in solution. The bis(tetrafluoroborate) salt, $[Pd(Ph_2Pqn)_2](BF_4)_2$ (**5**), which crystallizes in colorless needles, seems to exist as a square-planar dication, *cis*(*P*)-$[Pd(Ph_2Pqn)_2]^{2+}$. Although it was not possible to determine the crystal structure of **5**, the structure of *cis*(*P*)-$[Pd(Ph_2Pqn)_2]^{2+}$ was speculated from the crystal structures of yellow $Pd(Ph_2Pqn)_2Cl_2\cdot 2CH_2Cl_2\cdot H_2O$ (**1a**) and $Pd(Ph_2Pqn)_2Br_2\cdot$ 4.5MeOH (**2a**). Owing to the interligand steric repulsion between the mutually *cis*-positioned quinolyl groups, two quinolyl planes in *cis*(*P*)-$[Pd(Ph_2Pqn)_2]^{2+}$ are bent away from the Pd^{II} coordination plane, as observed for *cis*(*P*)-$[Pd(Me_2Pqn)_2](BF_4)_2$.[1]

The $Pd(Ph_2Pqn)_2Cl_2$ (**1**) and $Pd(Ph_2Pqn)_2Br_2$ (**2**) complexes deposited as either yellow (**1a** and **2a**) or orange (**1b** and **2b**) crystals, depending on the solvent used for crystallization. In the yellow crystals of **1a** and **2a**, the halide anions (Cl^- or Br^-) are located above and below the square-planar Pd^{II} coordination plane of *cis*-$[Pd(Ph_2Pqn)_2]^{2+}$. The Pd···Cl distances of 3.262(3) and 3.386(3) Å in **1a** and the Pd···Br distances of 3.432(2) and 3.505(2) Å in **2a** are too long to be treated as a typical coordination bond. However, the yellow color of the crystals strongly indicates the existence of a charge-transfer interaction between Pd^{II} and Cl^- or Br^-. When the crystals of **1a**, **1b**, **2a** or **2b** were dissolved in methanol, the complex seems to exist as dicationic species, *cis*(*P*)-$[Pd(Ph_2Pqn)_2]^{2+}$, without Pd^{II}···halide interaction. On the other hand, in dichloromethane it seems that these species exist as a monocationic complex with a bonding interaction between Pd^{II} and halide, $[Pd(Ph_2Pqn)_2Cl]^+$ or $[Pd(Ph_2Pqn)_2Br]^+$. Although the structures of such monocationic complexes in dichloromethane were not determined unambiguously, a possible structure was clarified by the crystal structure analysis of $[Pd(Ph_2Pqn)_2Cl]BF_4\cdot$MeOH (**4**·MeOH). In this crystal the Pd^{II} is surrounded by a chelating Ph_2Pqn, a monodentate P-donating Ph_2Pqn and a Cl atom in a highly distorted square-planar fashion with a typical Pd–Cl coordination bond. The N(21) atom in the uncoordinated quinolyl group was distant from Pd^{II}, Pd···N(21) 2.725(7) Å. It was also inferred that coordination of N(21) to Pd^{II} to form a trigonal bipyramidal five-coordinate complex is not energetically unfavorable. This complex **4** in acetonitrile exhibits a similar UV–vis and ^{31}P NMR spectra to those of complex **1** in dichloromethane. Since the ^{31}P NMR spectra of these complexes show a sharp single resonance at 30 °C, and since the single signal becomes broader at −40 °C, an exchange equilibrium as described in Scheme 2 may exist in solution.

Another type of coordination structure involving the Pd^{II}···halide interactions was revealed by the crystallographic study of the orange $Pd(Ph_2Pqn)_2Br_2\cdot$MeOH (**2b**). In **2b** one of the Br^- ions is located at the apical position of the square pyramidal $Pd^{II}P_2N_2Br$ moiety with an elongated Pd–Br bond of 3.0136(8) Å. In this cationic complex, $[Pd(Ph_2Pqn)_2Br]^+$, two Ph_2Pqn ligands were not equivalent; one of the Ph_2Pqn ligand forms a short Pd–N bond with a quinolyl ring co-planar to the Pd^{II} coordination plane, while the other quinolyl ring is largely dislocated from the Pd^{II} plane with a relatively long Pd–N bond. Hence, the elongated square-pyramidal structure found in **2b** may correspond to the intermediate for the ligand exchange process of *cis*(*P*)-$[PdX(Ph_2Pqn\text{-}\kappa P,N)(Ph_2Pqn\text{-}\kappa P)]^+$ (Scheme 2).

It was also important to comment on the structural and color differences between the present Pd^{II} complexes with Ph_2Pqn ligands and $[Pd(R_2PCH_2CH_2NH_2)_2Cl]BF_4$ complex (R = Me or Ph).[20] The aminoethylphosphine complexes are colorless, with an elongated square-pyramidal coordination geometry in which the Pd–Cl bond is 3.156(3) Å. Although this distance is far longer than the typical Pd–Cl coordination bond, it is shorter than those in **1a** that exhibits a yellow color. Therefore, the charge-transfer interaction between Pd^{II} and Cl^-, which is responsible for the yellow color of **1a**, is not simply related to the Pd···Cl distance. For the bis(Ph_2Pqn) complex with a *cis* configuration, *cis*-$[Pd(Ph_2Pqn)_2]^{2+}$, a severe steric repulsion between the mutually *cis*-positioned quinolyl groups forces the quinolyl N-donor orbital away from the direction of the Pd^{II} center. As the energy of the Pd^{II} LUMO ($d_{x^2-y^2}$) orbital is lowered by this distortion, the energy that corresponds to the charge-transfer from Cl^- to Pd^{II} $d_{x^2-y^2}$ becomes smaller. Furthermore, this distortion may also be responsible for the catalytic activity of $Pd(Ph_2Pqn)_2XY$ complexes for ethylene polymerization reactions,[4] since the bonding between Pd^{II} and quinolyl-N should be labile enough to promote the coordination of olefins.

The author is grateful to Professors Hideo D. Takagi (Nagoya University) and Kazuo Kashiwabara (Nagoya University) for valuable discussions and comments, and to Mr. Seiji Adachi (Osaka University) for VT ^{31}P NMR measurements. This work was partly supported by a Grant-in-Aid for Scientific Research (No. 16550055) from the Ministry of Education, Culture, Sports, Science and Technology.

References

1 T. Suzuki, K. Kashiwabara, and J. Fujita, *Bull. Chem. Soc. Jpn.*, **68**, 1619 (1995).

2 H. A. Hudali, J. V. Kingston, and H. A. Tayim, *Inorg. Chem.*, **18**, 1391 (1979).

3 T. Suzuki, T. Kuchiyama, S. Kishi, S. Kaizaki, and M. Kato, *Bull. Chem. Soc. Jpn.*, **75**, 2433 (2002); T. Suzuki, T. Kuchiyama, S. Kishi, S. Kaizaki, H. D. Takagi, and M. Kato, *Inorg. Chem.*, **42**, 785 (2003).

4 W.-H. Sun, Z. Li, H. Hu, B. Wa, H. Yang, N. Zhu, X. Leng, and H. Wang, *New J. Chem.*, **26**, 1474 (2002); T. Suzuki, S. Kaizaki, and F. Okuda, Jpn. Kokai Tokkyo Koho, JP 2002080522 (2002).

5 P. Wehman, H. M. A. van Donge, A. Hagos, P. C. J. Kamer, and P. W. N. M. van Leeuwen, *J. Organomet. Chem.*, **535**, 183 (1997).

6 P. Espinet and K. Soulantica, *Coord. Chem. Rev.*, **193–195**, 499 (1999); C. S. Slone, D. A. Weinberger, and C. A. Mirkin, *Prog. Inorg. Chem.*, **48**, 233 (1999).

7 D. G. Allen, G. M. McLaughlin, G. B. Robertson, W. L. Steffen, G. Salem, and S. B. Wild, *Inorg. Chem.*, **21**, 1007 (1982).

8 G. Salem and S. B. Wild, *Inorg. Chem.*, **31**, 581 (1992).

9 K. Issleib and K. Hörnig, *Z. Anorg. Allg. Chem.*, **389**, 263 (1972); K. Issleib and M. Z. Haftendorn, *Z. Anorg. Allg. Chem.*, **376**, 79 (1971).

10 R. D. Feltham and H. G. Metzger, *J. Organomet. Chem.*, **33**, 347 (1971).

11 J. R. Doyle, P. E. Slade, and H. B. Jonassen, *Inorg. Synth.*, **6**, 216 (1960).

12 P. Coppens, L. Leiserowitz, and D. Rabinovich, *Acta Crystallogr., Sect. A*, **18**, 1035 (1965).

13 "PROCESS-AUTO, Automatic Data Acquisition and Processing Package for Imaging Plate Diffractometer," Rigaku Corporation, Tokyo, Japan (1998).

14 T. Higashi, "ABSCOR, Empirical Absorption Correction Based on Fourier Series Approximation," Rigaku Corporation, Tokyo, Japan (1995).

15 A. Altomare, G. Cascarano, C. Giacovazzo, A. Guagliardi, M. C. Burla, G. Polidori, and M. Camalli, *J. Appl. Crystallogr.*, **27**, 435 (1994).

16 G. M. Sheldrich, *Acta Crystallogr., Sect. A*, **46**, 467 (1990); G. M. Sheldrich, "SHELXL97," University of Göttingen, Germany (1997).

17 Molecular Structure Corporation and Rigaku Co. Ltd., "TeXsan, Single Crystal Structure Analysis Software, Ver. 1.9," The Woodlands, TX, USA and Akishima, Tokyo, Japan (1998).

18 R. H. Lee, E. Griswold, and J. Kleinberg, *Inorg. Chem.*, **3**, 1278 (1964); T. Suzuki, S. Kaizaki, and K. Kashiwabara, *Inorg. Chim. Acta*, **298**, 131 (2000).

19 A. G. Orpen, L. Brammer, F. H. Allen, O. Kennard, D. G. Watson, and R. Taylor, *J. Chem. Soc., Dalton Trans.*, **1989**, S1.

20 T. Suzuki, A. Morikawa, and K. Kashiwabara, *Bull. Chem. Soc. Jpn.*, **69**, 2539 (1996).

21 In the crystal structure of **2b**, the N(1) atom was displaced by 0.746(4) Å from the least-squares PdP_2N_2 plane, while the other atoms were on the plane within 0.114(4) Å.

22 P. Sevillano, A. Habtemariam, A. Castineiras, M. E. García, and P. J. Sadler, *Polyhedron*, **18**, 383 (1999).

23 K. M. Chui and H. M. Powell, *J. Chem. Soc., Dalton Trans.*, **1974**, 1879, 2117.

24 For example: A. Miedaner, R. C. Haltiwanger, and D. L. DuBois, *Inorg. Chem.*, **30**, 417 (1991); L. M. Engelhardt, J. M. Patrick, C. L. Raston, P. Twiss, and A. H. White, *Aust. J. Chem.*, **37**, 2193 (1984).

25 S.-I. Aizawa, T. Iida, and S. Funahashi, *Inorg. Chem.*, **35**, 5163 (1996); R. E. Marsh, *Acta Crystallogr., Sect. B*, **55**, 931 (1999).

26 The halide coordination/uncoordination equilibrium, i.e., square-planar *cis*(*P*)-$[Pd(Ph_2Pqn)_2]^{2+}$ + X^-/square pyramidal (*SPY*-5-13)-$[PdX(Ph_2Pqn)_2]^+$, would also be possible for this fluxionality.